

Effect of Reduced Aortic Compliance on Cardiac Efficiency and Contractile Function of In Situ Canine Left Ventricle

Raymond P. Kelly, Richard Tunin, and David A. Kass

This study tests the hypothesis that arterial vascular stiffening adversely influences in situ left ventricular contractile function and energetic efficiency. Ten reflex-blocked anesthetized dogs underwent a bypass operation in which a Dacron graft was sewn to the ascending aorta and connected to the infrarenal abdominal aorta via a plastic conduit. Flow was directed through either native aorta or plastic conduit by placement of vascular clamps. Arterial properties were measured from aortic pressure–flow data, and ventricular function was assessed by pressure–volume (PV) relations. Coronary sinus blood was drained via an extracorporeal circuit for direct measurement of myocardial O₂ consumption (M \dot{V} O₂). Data at multiple steady-state preload volumes were combined to derive chamber function and energetics relations. Energetic efficiency was assessed by the inverse slope of the M \dot{V} O₂–PV area relation. Directing flow through plastic versus native aorta resulted in a 60–80% reduction in compliance but little change in mean resistance. Arterial pulse pressure rose from 34 to 99 mm Hg ($p < 0.001$). Contractile function assessed by the end–systolic PV relation, stroke work–end–diastolic volume relation, and dP/dt_{max} at matched end–diastolic volume did not significantly change. However, M \dot{V} O₂ increased by 32% ($p < 0.01$) and was matched by a rise in PV area, such that the M \dot{V} O₂–PV area relation and efficiency was unaltered. The M \dot{V} O₂ required to sustain a given stroke volume, however, increased from 20% to 40%, depending on the baseline level ($p < 0.001$). Thus, whereas the contractile function and efficiency of normal hearts are not altered by ejection into a stiff vascular system, the energetic cost to the heart for maintaining adequate flow is increased. This suggests a mechanism whereby human vascular stiffening may yield little functional decrement at rest but limit reserve capacity under conditions of increased demand. (*Circulation Research* 1992;71:490–502)

KEY WORDS • aortic input impedance • ventriculovascular coupling • myocardial energetics • pressure–volume relations • ventricular function

Human aortas undergo progressive degeneration due to normal aging^{1–7} and disease processes such as chronic hypertension.^{8,9} The dominant change is that of reduced vascular distensibility, which has an impact on measures of arterial properties such as the shape of the arterial pressure and flow wave,^{5,10} aortic input impedance spectra,^{5,8,11} and pulse-wave velocity.^{7,9,12} Although it is widely believed that these abnormalities of vascular load have adverse effects on cardiac contractile function and energetic efficiency,^{12–14} this hypothesis has remarkably little direct supporting data.

For example, isolated canine heart studies have reported little change in the end-systolic pressure–volume

relation (ESPVR) despite twofold changes in total compliance, characteristic impedance, and resistance.¹⁵ Myocardial efficiency, defined by the relation between total pressure–volume work (pressure–volume area [PVA]) and oxygen consumption, has also been shown to be little influenced by vascular load or ejection history.^{16–18} We recently reported that lowering vascular resistance could have positive effects on both contractility and efficiency¹⁹; however, the relevance of this finding to in situ hearts ejecting into a stiff vasculature is unknown. Other prior studies have attempted to measure in situ effects of aortic stiffening on cardiac function and energetics by replacing the aorta with an artificial conduit or by physically stiffening the native aorta.^{20–23} However, these data largely focused on vascular properties, providing little direct assessment of ventricular performance or energetics. Furthermore, none of these studies demonstrated increased myocardial oxygen consumption (M \dot{V} O₂) from ejection into a stiffened aorta.^{22,23} Thus, despite the popularity of the notion that vascular stiffening adversely affects cardiac contractility and energetics, confirmation with precise measurements of the magnitude of this interaction has not been made.

The purpose of the present study was to determine in situ whether acutely reduced vascular compliance sig-

From the Division of Cardiology, Department of Internal Medicine, The Johns Hopkins Medical Institutions, Baltimore, Md.

Supported by a grant-in-aid from the Maryland Chapter of the American Heart Association, Physician Scientist Award HL-18120 from the National Institutes of Health (D.A.K.), the National Heart Foundation of Australia, the Royal Australasian College of Physicians, and a Fulbright grant (R.P.K.). D.A.K. is an Established Investigator of the American Heart Association.

Address for correspondence: David A. Kass, MD, Division of Cardiology, Carnegie 565B, Johns Hopkins Medical Institutions, 600 N. Wolfe Street, Baltimore, MD 21205.

Received July 1, 1991; accepted April 14, 1992.

nificantly alters ventricular contractility, $\dot{M}\dot{V}O_2$, or efficiency. Pressure–volume analysis was used to assess chamber properties and energetics. A novel surgical preparation was developed in which virtually the entire canine thoracic aorta was bypassed by a stiff plastic conduit and the ventricular outflow was directed through either the native or stiff aortas. Total $\dot{M}\dot{V}O_2$ was directly measured and compared with simultaneous pressure–volume data for efficiency calculations. These data provide the first direct in situ evidence confirming energetic consequences but insignificant systolic contractile effects from cardiac ejection into a stiff vascular system.

Materials and Methods

Preparation

Ten adult mongrel dogs (30–35 kg) were anesthetized with pentobarbital (30 mg/kg i.v.). The dogs were pretreated with 100 mg i.m. hydrocortisone and 50 mg p.r. indomethacin before study, which served to stabilize the preparation during extracorporeal blood circulation. The animals were intubated and ventilated on a volume respirator with 40% enhanced inspired oxygen. Ventilation was guided by arterial blood gases obtained every 30–60 minutes.

Both carotid and femoral arteries were cannulated by fluid-filled catheters to allow arterial blood sampling and pressure monitoring and to provide a route for cerebral perfusion after aortic bypass. The right femoral vein was cannulated for intravenous fluid, blood, and drug administration. The animals underwent a midster-notomy and midline abdominal incision. The inferior and superior vena cavae and the descending thoracic aorta at the level of the diaphragm were snared with umbilical ties. The pericardium was opened, and the heart was suspended in a pericardial cradle (Figure 1). The proximal aortic root was carefully dissected free from surrounding connective and fatty tissue, and the right brachiocephalic artery was tied off and divided. A 6F micromanometer catheter (presoaked for 2 hours at room temperature and calibrated to a mercury manometer) was inserted through a purse-string suture in the high left ventricular free wall to monitor intracavity pressure (site A in Figure 1). Distal (femoral artery) perfusion pressure was monitored using a fluid-filled line connected to a Statham gauge.

The proximal ascending aorta was partially occluded with an aortic clamp at or just proximal to the origin of the brachiocephalic artery. This isolated a portion of the aortic wall (site B) onto which a 2–3-cm long Dacron vascular graft was sewn by end-to-side anastomosis using a pair of running 4–0 prolene sutures. With the aorta appropriately clamped, there was minimal rise in left ventricular pressure, and distal perfusion was well maintained. The Dacron graft (18 or 14 mm o.d.) was matched to the size of the proximal aorta. After partial unclamping of the aortic wall to ensure adequate hemostasis, the suture line was stabilized with felt pledgets and collagen fiber (Avitene, MedChem Prod. Inc., Woodburn, Mass.), and the aorta was left partially clamped to enable a thrombotic seal to form at the anastomosis.

The abdominal aorta was then dissected free from surrounding tissue, cross-clamped just above the iliac

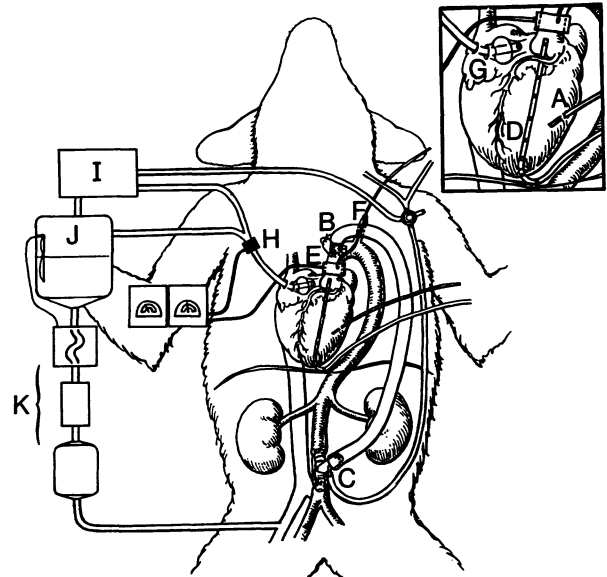


FIGURE 1. Schematic diagram of the canine surgical bypass preparation. A, Left ventricular micromanometer; B, Dacron anastomosis site on the ascending aorta; C, abdominal aorta connection of Tygon bypass tube; D, conductance catheter for left ventricular volume; E, proximal aortic flow probe; F, central aortic micromanometer; G, balloon-tipped catheter for total drainage of coronary sinus blood; H, in-line flow probe; I, arteriovenous blood oxygen content difference analyzer; J, blood drainage reservoir with servo-controlled fluid level; K, parastaltic pump, blood filter, and heat exchanger from which blood was returned to a femoral vein. Placement of occlusion clamps on the Tygon conduit at proximal and distal anastomoses directed flow down the native aorta. Repositioning clamps around the native aorta at the diaphragm and just beyond the proximal anastomosis (near site F) directed flow down the Tygon conduit.

bifurcation, and partially transected to allow insertion of a short T-tube cannula (site C in Figure 1). This was secured in place with umbilical tape. Heparin (5,000 units) was administered intravenously. The common port of the T-tube cannula was clamped off, distal perfusion was restored, and the abdomen was closed with surgical clamps.

A purse-string suture was placed at the left ventricular apex, and an 8F multielectrode conductance catheter was advanced through the apex and extended to a position just above the aortic valve (by monitoring intraluminal pressure) (site D in Figure 1). The catheter was attached to a signal generator/processor (Sigma V, Leycom, The Netherlands), which provided an excitation current at base and apical electrodes and measured voltages between intervening electrode pairs along the catheter. These voltages were related to chamber blood volume as previously described.^{24,25} Examination of individual pressure–volume segment loops determined which electrodes were intracavity (counterclockwise loop), and electronic switching (i.e., eliminating segments within the aortic root from the total volume calculation) enabled the appropriate electrodes to be used. Once the catheter was correctly positioned, it was secured by the apical purse-string suture.

An ultrasonic flow probe (Transonics, Ithaca, N.Y.) (site E in Figure 1) was placed around the aortic root within 2 cm of the aortic valve and immediately below the Dacron anastomosis (site B). A 6F micromanometer catheter was inserted via the left brachiocephalic artery (site F) and secured in place so that the catheter tip lay just downstream from the aortic flow probe. Since both aortic arch branches were now ligated, head perfusion was maintained by flow diverted from the abdominal aorta using a perfusion line connecting a side port of the abdominal aortic cannula to the carotid cannula.

The right atrial appendage was cannulated with a modified 14F Foley (urinary drainage) catheter by using a thin slightly angled metal obturator to assist passage. The catheter was advanced into the proximal coronary sinus (CS), and the balloon was inflated with 3–4 ml saline so that it fit snugly in the CS orifice (site G). The catheter was secured in place with a proximal tie around the right atrial appendage. With the metal obturator removed, CS blood was allowed to drain by gravity through an in-line ultrasound volume flow probe (site H) (Transonics), and a portion of the CS blood was diverted to a blood oxygen content difference analyzer (site I). Residual CS blood (plus outflow from the blood analyzer) was drained by gravity into a reservoir (site J). The reservoir blood was pumped by peristaltic pump through a heat exchanger (37°C), air trap, and arterial filter (site K) and returned to the right femoral vein. A custom electronic switching device detected the upper fluid level of blood in the reservoir and provided feedback control to the pump. The fluid level could be raised or lowered to allow changes in steady-state venous return and cardiac preload. After completion of the CS drainage circuit, an additional 5,000 units heparin was administered.

The distal abdominal and proximal aortic cannulas were connected by a 58-cm (0.5-in.-i.d., 0.625-in.-o.d.) plastic tube (Tygon, Norton, Akron, Ohio) with a compliance of 3×10^{-3} ml/mm Hg over the physiological pressure range. Any residual air was removed from the tube, and then the proximal aortic clamp was removed to allow flow to proceed in parallel through both the native aorta and Tygon conduit. After establishing the stability of the preparation, the plastic conduit was then reclamped both proximally and distally to provide native aortic flow only.

Protocol

At least 10 minutes was allowed for stabilization after the preparation was completed. Pharmacological support of blood pressure and contractility was required in some dogs and was provided by low dose infusion of epinephrine (1–3 μ g/kg per minute). Reflex blockade was achieved by hexamethonium HCl (10 mg/kg) and assessed by lack of heart rate change with varying load and transient cessation of carotid flow. Additional hexamethonium (5 mg/kg) was administered if required.

Left ventricular outflow was directed through either the native aorta or Tygon conduit by placement of vascular occlusion clamps. Flow through the native aorta was achieved by clamping off the Tygon conduit at the proximal and distal connections. Flow through the Tygon conduit was obtained by clamping the native aorta immediately beyond the proximal anastomosis (mid ascending aorta) and at the diaphragm. This latter

site was chosen to avoid hemodynamic effects of renal or bowel ischemia. Multiple steady-state pressure–volume, aortic pressure–flow, coronary sinus flow, and arteriovenous oxygen difference data were obtained at varying preload volumes. Preload was reduced in gradual steps by slowing the speed of the pump returning blood from the CS drainage reservoir (site K in Figure 1). With each load change, all variables were allowed to equilibrate for 1–2 minutes before recording. Once a set of data (four to seven preload volumes) was obtained for either the native aorta or Tygon conduit, the clamps were repositioned so that flow was directed via the alternate route. After several minutes for stabilization, the protocol and measurements were repeated. In addition to steady-state data, pressure–volume loop data were also obtained during acute transient preload reduction by applying traction to inferior and superior vena caval snares.

Data were monitored on an eight-channel chart recorder and displayed with custom-developed data acquisition/display software using an Intel 286 processor-based microcomputer. Data were digitally recorded at 200 Hz and stored on removable hard drives for subsequent analysis.

At the end of the study, the animals were euthanized by pentobarbital overdose and potassium chloride cardioplegia. The CS drainage catheter placement and balloon seal were assessed by injection of monastral blue dye retrogradely down the CS catheter lumen (before cardioplegia) to test for leakage into the right atrium and by direct postmortem inspection. The heart was removed from the chest, and right and left ventricles (free wall plus septum) were weighed.

Volume Signal Calibration

Conductance catheter volumes were calibrated to the aortic flow probe by determining the ratio of integrated flow to catheter-derived stroke volume (SV). This gain was calculated for each steady-state beat (coefficient of variation, 6.2%) in a given preload run, and the results were averaged to obtain a mean calibration gain. Variation in mean gain between native and Tygon data runs averaged 11%; however, this as well as interanimal differences did not affect the results, since a new mean gain was determined and applied to each preload data set. The conductance signal also includes an offset, which is primarily due to cardiac muscle conductance. Estimation of this offset was not made in the present study, since the focus was on relative changes due to rapidly altered vascular properties in the same heart. Furthermore, the primary function parameters such as stroke work (SW), SV, and PVA are not influenced by a volume offset.

Data Analysis

Ventricular systolic function. Data from multiple steady-state preloads were combined to determine systolic and diastolic pressure–volume relations. Left ventricular contractile function was assessed by ESPVR, the SW–end-diastolic volume (V_{ed}) relation, and the maximal rate of pressure rise (dP/dt_{max}) at a common V_{ed} . The ESPVR was fit by linear regression (using an iterative algorithm²⁶) to obtain a slope and volume intercept (V_0). SW was the digitally integrated area of each pressure–volume loop and was plotted versus V_{ed}

(volume at the lower right corner of the loop) to generate the $SW-V_{ed}$ relation. These relations were highly linear and fit by least-squares regression. The time derivative of ventricular pressure was digitally calculated by a running weighted five-point slope. dP/dt_{max} was compared for native versus Tygon aortas at a matched V_{ed} to minimize loading effects.

Myocardial energetics. Myocardial energetics was assessed by analysis of the relation between left ventricular $M\dot{V}O_2$ per beat and total pressure–volume work (PVA) as described by Suga.^{16,17} We also examined the relation between $M\dot{V}O_2$ per beat and cardiac SV to assess the oxygen cost of maintaining or increasing SV (or cardiac output) while ejecting into a stiffer arterial system. Over a physiological range of mean vascular pressures, cardiovascular reserve capacity is closely tied to the ability of the system to enhance cardiac output, making this relation important.

$M\dot{V}O_2$ was calculated from the product of coronary sinus blood flow and arteriovenous oxygen difference. PVA is the sum of SW plus the area bounded by the ESPVR and diastolic pressure–volume relations between end-systolic volume and V_o . V_o was determined by linear extrapolation of the ESPVR, with an average standard error of the estimate of 3.1 ml. To obtain the non-SW portion of PVA, the diastolic data were fit by nonlinear regression, and the area between diastolic and systolic pressure–volume relations was determined by analytical integration.¹⁹ $M\dot{V}O_2$ –PVA relations were fit by linear regression. The slope provides a measure of chemomechanical transduction efficiency, and the offset provides O_2 consumption for basal metabolism and excitation–contraction coupling.

This study examined effects of altered arterial load on left ventricular performance; therefore, total $M\dot{V}O_2$ was adjusted to reflect left ventricular $M\dot{V}O_2$ only. This was done by assuming that the $M\dot{V}O_2$ values in right and left ventricles were proportional to their masses (linking the septum with the left ventricle). Thus, $M\dot{V}O_2$ was multiplied by the ratio of left ventricular/(left ventricular+right ventricular) weight. Finally, to compare $M\dot{V}O_2$ –PVA relations between hearts, both $M\dot{V}O_2$ and PVA were normalized to 100 g left ventricular weight as described by Suga.¹⁶

Vascular properties. Arterial properties were assessed from ascending aortic pressure–flow measurements. Impedance spectra from steady-state beats were obtained by discrete Fourier series analysis. Total mean resistance was the zero-order term from the impedance spectra, and characteristic impedance was the average modulus from 5 to 12 Hz. Flow signal noise was assessed by assuming a zero flow level during late diastole and determining the amplitude of fluctuations during this period (by Fourier analysis). Frequency coefficients that did not exceed this level were not included in the analysis. Peripheral resistance based on a three-element Windkessel model was estimated as the difference between total mean resistance and characteristic impedance.

Total vascular compliance was estimated using the method of Liu et al.²⁷ This approach, also based on the Windkessel model, calculates arterial compliance from the area under the diastolic pressure waveform rather than from nonlinear fits. Thus, total vascular compliance equals $A_{21}/R_a(P_1-P_2)$ (Equation 11 in Reference 27), where A_{21} is the area under the diastolic pressure wave

between two arbitrary time points (1 and 2), and P_1-P_2 is the corresponding pressure difference. Since diastolic waveforms rarely followed a pure monoexponential decay and also displayed wave oscillations, particularly in native aorta data, total vascular compliance estimates varied with the portion of diastole (position of time points 1 and 2) used in this calculation. An upper range estimate was obtained using the entire diastolic period (i.e., P_1 is incisura pressure, and P_2 is end-diastolic pressure). A lower range estimate was obtained by positioning P_1 at the peak of any reflected wave, so that only a monotonic declining portion remained. Both estimates are reported.

In addition to steady-state data, a subset of hearts underwent random pacing to obtain broadband impedance spectra. Atrial pacing leads were attached, and a random number generator was used to obtain cycle lengths between 250 and 1,200 msec. Pacing data were continuously recorded at 100 Hz for 4 minutes. Data were divided into eight contiguous bins (2,048 points, or 10 seconds per bin), windowed using a Hanning filter, analyzed by fast Fourier transform, and averaged in the frequency domain to yield impedance spectra. Modulus, phase, and coherence were determined at each frequency.

Statistical analysis. All data are presented as mean±SD. Steady-state variables were compared by paired *t* tests, with statistical significance accepted at $p<0.05$. Linear regression slopes and offsets for the various relations (e.g., end-systolic pressure versus end-systolic volume; $M\dot{V}O_2$ versus PVA; SW versus V_{ed}) were also compared by paired *t* tests. In addition, all of the raw data for each relation was combined into a single multiple-regression model²⁸ to provide a more robust assessment for differences. The model included dummy variables coding for the aorta type and for variability of slope and offset among individual dogs. The output provided the mean relation for both the native and Tygon aorta and a determination of whether aorta type significantly altered either mean slope or offset. Numerical analysis was performed on an Intel 386 processor-based microcomputer using custom-designed software and a commercial statistics package (SYSTAT, Inc., Evanston, Ill.).

Results

Aortic Impedance and Pressure–Flow and Pressure–Volume Contours

Diversion of flow from the native aorta to the Tygon conduit resulted in a dramatic increase in several measures of pulsatile arterial load (Table 1). Arterial systolic pressure and pulse pressure increased by 51.8 mm Hg (+47%) and 64.8 mm Hg (+190%), respectively (both $p<0.01$). Arterial diastolic pressure decreased slightly, yielding a net +11 mm Hg increase in mean pressure. Cardiac output was not significantly altered. Data provided in Table 1 were obtained at steady state, with the blood return flow rate adjusted to maintain a similar volume level in the external reservoir.

Figure 2 displays an example of aortic pressure and flow waveforms and ventricular pressure–volume loops for flow through native and Tygon “aortas,” as well as intermediate combinations. The examples on the left show flow through the native aorta only, revealing a narrow pulse pressure, rounded arterial waveform, early

TABLE 1. Mechanical, Vascular, and Energetic Consequences of Switch to Stiff (Tygon) Aorta

Variable	Native aorta	Tygon conduit	<i>p</i>
Vascular			
P_{sys} (mm Hg)	109.8±18.6	161.6±34.9	<0.001
P_{dia} (mm Hg)	75.7±18.1	62.7±17.9	<0.01
P_{mean} (mm Hg)	91.7±20.5	102.6±22.5	<0.05
PP (mm Hg)	34.1±8.3	98.9±24.8	<0.001
R_{T} (mm Hg · ml ⁻¹ · sec ⁻¹)	3.04±1.5	3.66±1.05	<0.05
R_{C} (mm Hg · ml ⁻¹ · sec ⁻¹)	0.27±0.11	0.41±0.17	<0.05
R_{A} (mm Hg · ml ⁻¹ · sec ⁻¹)	2.77±1.4	3.24±0.92	NS
C_{A} (ml/mm Hg)	1.65±0.85–0.63±0.38*	0.19±0.07–0.11±0.08*	<0.001
Ventricular			
P_{es} (mm Hg)	104.7±23.1	153.4±31.5	<0.001
P_{ed} (mm Hg)	6.8±2.4	9.4±3.8	<0.05
CO (l/min)	1.9±0.55	1.7±0.44	NS
EF (%)	50.4±12.5	42.1±13.4	NS
HR (bpm)	119.5±9.8	121.1±12.8	NS
SW (mm Hg · ml)	1,572.8±482.4	1,630.4±425.3	NS
$V_{\text{ed}}-V_{\text{o}}$ (ml)	35.6±14.5	40.2±18.3	0.18
$V_{\text{es}}-V_{\text{o}}$ (ml)	19.1±11.3	25.9±15.1	<0.05
Energetics			
$M\dot{V}O_2$ (ml O ₂ · 100 g ⁻¹ · beat ⁻¹)	0.102±0.03	0.135±0.049	<0.01
PVA (mm Hg · ml/100 g)	2,498.8±863.7	3,450.1±1,547.3	<0.05
EFF			
SW/ $M\dot{V}O_2$ (%)	22.9±10.9	17.6±5.4	0.052
1/ α (%)	35.5±11.2	34.4±9.1	NS

P_{sys} , P_{dia} , and P_{mean} , arterial systolic, diastolic, and mean pressure, respectively; PP, pulse pressure; R_{T} , total mean resistance; R_{C} , characteristic impedance; R_{A} , peripheral resistance; C_{A} , total compliance; P_{es} and P_{ed} , ventricular end-systolic and end-diastolic pressure, respectively; CO, cardiac output; EF, ejection fraction, calculated as stroke volume/(end-diastolic volume [V_{ed}]-volume intercept [V_{o}]); HR, heart rate; bpm, beats per minute; SW, stroke work; V_{es} , end-systolic volume; $M\dot{V}O_2$, myocardial oxygen consumption; PVA, pressure-volume area; EFF, efficiency; α , slope of $M\dot{V}O_2$ -PVA relation.

*Upper and lower range estimates for compliance are provided. See "Materials and Methods."

rapid flow peak, and the square shape of the pressure-volume loop. The next set of examples to the right shows data with flow permitted down both native and Tygon aortas. There was no difference between these data and the waveforms obtained with flow through the native aorta only. This indicates that wave reflections arising from the proximal Dacron conduit or abdominal T-tube connectors were of little influence when flow continued in the native aorta. Clamping the native aorta at the diaphragm while maintaining flow through the Tygon conduit (distal Ao in the figure) resulted in a late-systolic wave reflection, elevating systolic pressures midway into ejection. Repositioning the native clamp proximally (just beyond the Tygon anastomosis) yielded a very different response (far right examples), characterized by a marked widening of the pulse pressure and continuously rising systolic pressures with a late systolic peak. This last configuration achieved the greatest reduction in net vascular compliance and was therefore used for comparison with native aortic flow.

Figure 3 shows typical impedance spectra (modulus and phase) derived from steady-state (left panels) and random-paced (right panels) aortic pressure-flow data for both native (solid line) and Tygon (dashed line) aortas. The moduli for flow through the native aorta rapidly declined to low amplitudes with an early zero-phase crossover. When flow was directed through

the Tygon aorta, the modulus decline was more gradual, with a rightward shift of the first modulus minimum and zero-phase crossover frequency. These changes were observed in both the steady-state and random-paced (pseudo-white noise) analyses and are consistent with reduced compliance from the Tygon aorta. Note that the moduli in the random-pacing analysis were normalized to the mean term to better display oscillations at the low frequencies. The coherence for the impedance spectra was near 1.0 up to 12 Hz and then slowly declined, most notably for flow via the Tygon conduit.

These examples were typical of the group changes in vascular loading induced by the switch to a stiff aorta (Table 1). Mean arterial pressure rose slightly from 91.7±20.5 to 102.6±22.5 mm Hg, whereas mean flow (cardiac output) did not significantly change. There was a 20% increase in total mean resistance as well as a rise in characteristic impedance (from 0.27±0.11 to 0.41±0.17 mm Hg · ml⁻¹ · sec⁻¹). The most prominent change, however, was a substantial reduction in total vascular compliance. As described in "Materials and Methods," two compliance estimates were made: an upper value derived from the entire diastolic pressure data and a lower value derived from data beyond the peak of any diastolic pressure oscillations. For the native aorta data, the upper estimate was 1.6 ml/mm Hg, and the lower estimate was

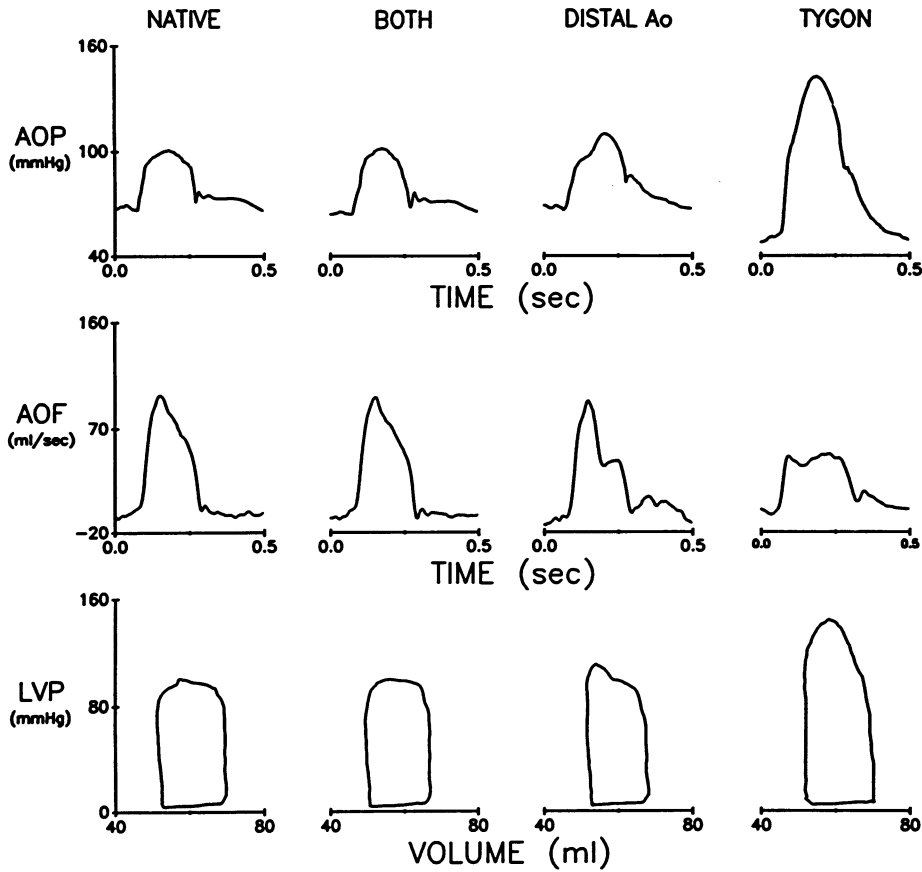


FIGURE 2. Typical examples of aortic pressure (AOP) waveforms (top panels), aortic flow (AOF) waveforms (middle panels), and left ventricular pressure (LVP)-volume loops (bottom panels) under varying bypass conditions. Conditions shown (from left to right) are as follows: native, only flow through native aorta; both, flow through both native and Tygon aortas; distal Ao, flow through Tygon aorta with the native aorta clamped at the diaphragm; and Tygon, flow through Tygon aorta only, with the native aorta clamped just distal to the ascending aorta anastomosis.

0.7 ml/mm Hg. Despite this range, total compliance with the Tygon aorta was significantly and markedly reduced (0.1–0.2 ml/mm Hg) by 60% to 80%.

The impedance changes with Tygon flow did not result from the small rise in mean arterial pressure. By using loops at slightly reduced preloads, Tygon data were ob-

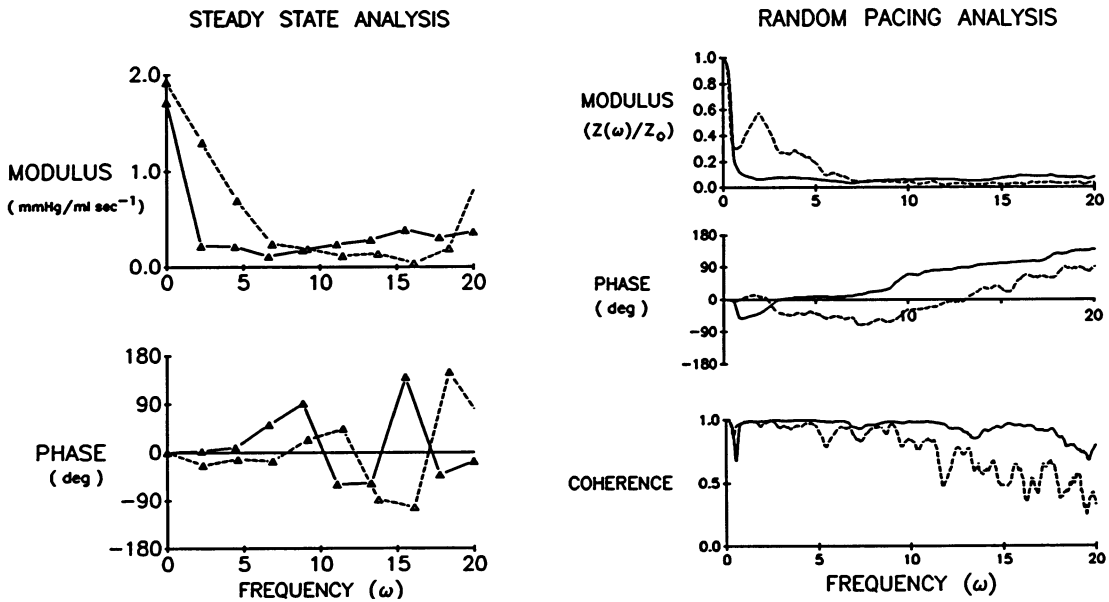


FIGURE 3. Graphs showing examples of impedance spectra obtained from signal-averaged steady-state beat analysis (left panels) and from random-pacing (white noise) analysis (right panels). In the right upper panel, impedance modulus $Z(\omega)$ is shown normalized to the zero order (mean) term (Z_0). Data for native aortic flow are represented by the solid lines, and data for the Tygon conduit are represented by the dashed lines. Both analyses revealed a more gradual initial decline of impedance modulus in the low frequency range and rightward shift of the first zero-phase crossover point when flow was directed through the stiff (Tygon) conduit. In this example, the characteristic impedance did not significantly differ between the two interventions. On average, there was a small but significant increase in characteristic impedance with flow through the Tygon conduit.

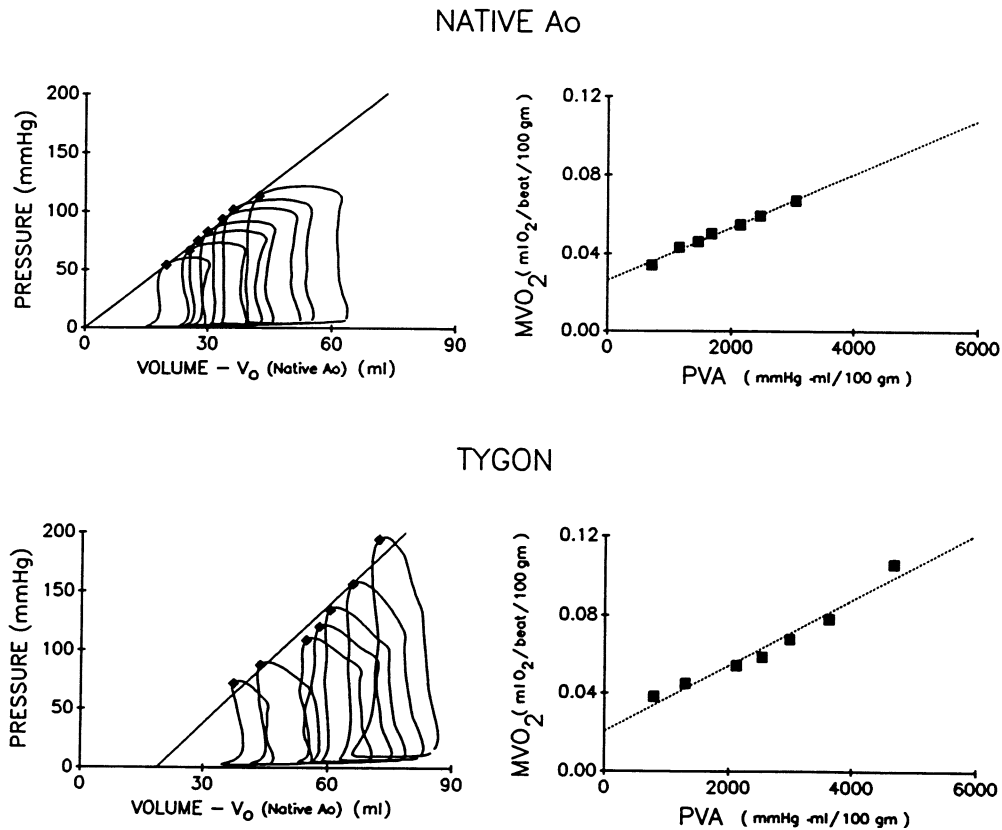


FIGURE 4. Graphs showing end-systolic pressure–volume relations (left panels) and myocardial oxygen consumption (MVO_2)–pressure–volume area (PVA) relations (right panels) for a single dog (No. 5 in Tables 2 and 4) with flow through the native aorta (Ao) versus the Tygon conduit. Volumes were adjusted by subtracting the volume intercept (V_o) derived from the native Ao end-systolic pressure–volume relation (ESPVR). There was a slight increase in the ESPVR slope in this example, although overall there was no significant change in this relation. Likewise, the MVO_2 –PVA relation was not altered by directing ventricular outflow through the stiff (Tygon) conduit.

tained with mean arterial pressure precisely matched to the native aorta flow data (mean pressure difference of $+0.3 \pm 4.5$ mm Hg). However, total peripheral resistance, compliance, and characteristic impedance values obtained from these beats (3.5 ± 1.1 mm Hg \cdot ml $^{-1} \cdot$ sec $^{-1}$, 0.13 ± 0.12 ml/mm Hg, and 0.44 ± 0.22 mm Hg \cdot ml $^{-1} \cdot$ sec $^{-1}$, respectively) were nearly identical to those derived from the beats at the slightly higher pressure (Table 1).

Ventricular Systolic Function

Steady-state ventricular function parameters are also provided in Table 1. Increasing the pulsatile load with flow through the Tygon aorta did not significantly change cardiac output, heart rate, ejection fraction, or SW. However, both end-systolic and end-diastolic pressures increased. There was a concomitant small increase in end-systolic volume and V_{ed} (provided in Table 1 as gain-adjusted volume minus V_o). The $V_{ed} - V_o$ change did not reach statistical significance, probably because of the lack of absolute volume calibration as well as statistical uncertainty in V_o estimation.

Pressure–volume relations (and MVO_2 –PVA relations) were obtained in nine of the 10 animals. In one animal, preload reduction during flow through the Tygon conduit resulted in diastolic coronary perfusion pressure of ≤ 40 mm Hg; therefore, the data were not used because of concern for potential cardiac ischemia. Figure 4 displays an example of pressure–volume and

MVO_2 –PVA data obtained during steady-state reductions in circulating blood volume. ESPVRs (left graphs) were linear and, in this case, showed a slight slope increase with flow through the Tygon aorta. For this example, the SW– V_{ed} relation slope was 59.5 mm Hg for native aorta versus 45.7 mm Hg for Tygon aorta, and dP/dt_{max} at a matched V_{ed} was also slightly less (1,301.7 versus 1,042.5 mm Hg/sec).

Group ESPVR data are provided in Table 2. There was no significant change in slope or offset (V_o) when flow was diverted through the Tygon conduit. This result in part reflected variable responses among experiments. Multivariate regression analysis yielded an average ESPVR of $P_{es} = 6.7(V_{es} - 47.0)$, where P_{es} is end-systolic pressure and V_{es} is end-systolic volume, for native aorta ($r^2 = 0.98$, $n = 49$) versus $P_{es} = 6.98(V_{es} - 42.8)$ for Tygon aorta ($r^2 = 0.93$, $n = 43$) ($p = NS$ for slope and V_o comparison between aortas). The V_o is large in these relations primarily from the uncorrected parallel conductance offset of the volume signal. Steady-state dP/dt_{max} matched to the same V_{ed} also did not significantly differ between the two data sets ($1,400.6 \pm 495$ versus $1,702.5 \pm 638.7$ mm Hg/sec). SW– V_{ed} relations were slightly altered. Although the change was not significant by paired t test of the individual regressions (Table 3), combined multiregression analysis revealed a small but significant change that could be statistically fit by either a pure slope increase (from 74.2 ± 3.0 to 79.8 ± 2.1 mm Hg, $p = 0.008$) or pure V_o (leftward) shift (from

TABLE 2. Systolic Contractility Indexes With Native Versus Tygon Aorta

Dog No.	ESPVR			SW-V _{ed} relation			n
	E _{es}	V _o '	r	M _{SW}	V _{SW} '	r	
Native aorta							
1	2.8	22.2	0.970	60.8	46.5	0.999	5
2	6.5	23.6	0.998	73.4	34.9	0.999	5
3	6.4	61.3	0.997	59.0	70.2	0.999	5
4	9.0	37.5	0.994	70.2	47.0	0.990	6
5	2.8	89.6	0.994	61.7	114.2	0.997	7
6	7.9	84.5	0.875	105.3	98.0	0.992	5
7	6.0	25.9	0.981	68.9	38.2	0.996	5
8	11.7	33.2	0.912	99.2	42.2	0.999	4
9	7.6	58.6	0.991	65.4	69.1	0.992	7
Mean	6.74	48.48	0.968	73.77	62.26	0.996	5.4
SD	2.82	26.05	0.044	16.88	28.05	0.004	1.0
Tygon aorta							
1	3.1	29.8	0.944	46.6	46.8	0.919	7
2	10.0	20.7	0.976	90.2	32.1	0.983	4
3	5.9	46.8	0.653	93.2	67.1	0.932	3
4	15.3	48.7	0.935	142.3	49.8	0.931	4
5	3.6	102.7	0.970	42.8	122.3	0.995	7
6	5.6	85.3	0.803	78.1	103.5	0.920	5
7	7.8	20.8	0.840	86.3	36.5	0.760	4
8	4.6	10.8	0.930	84.2	36.5	0.999	4
9	8.4	56.4	0.966	67.8	70.4	0.999	5
Mean	7.14	46.88	0.891	81.28	62.78	0.938	4.78
SD	3.81	30.90	0.107	29.27	31.66	0.075	1.39

ESPVR, end-systolic pressure–volume relation; SW, stroke work; V_{ed}, end-diastolic volume; E_{es}, slope value for ESPVR; V_o', volume intercept for ESPVR; r, correlation coefficient; M_{SW}, slope value for the SW–V_{ed} relation; V_{SW}', volume intercept for SW–V_{ed} relation; n, number of points per regression.

62.6±2.6 to 57.8±1.9 ml, p=0.016). Regardless, this effect was small and probably of little physiological importance. Combining the results from all three indexes suggests that there was little to no significant change in systolic contractile function when the heart was made to eject into the stiff aortic conduit.

The above data were obtained with multiple preload volumes at steady state. Since this is an unusual loading pattern for in vivo studies, we also compared pressure–volume relations obtained by more typical transient load interventions (bicaval occlusion). The results (Ta-

ble 3) were consistent with the steady-state data, displaying no significant change from switching flow between native and Tygon aortas.

Myocardial Oxygen Consumption and Efficiency

Flow through the stiff aorta resulted in significant increases in steady-state MVO₂ of more than 30% (Table 1), which was matched by an increase in total pressure–volume work (PVA). An example of MVO₂–PVA relations is also displayed in Figure 4 (right graphs). There was virtually no change in the relation as a consequence of

TABLE 3. Comparison of Indexes of Cardiac Contractility Derived From Transient Preload Reduction (Simultaneous Inferior Vena Cava and Superior Vena Cava Occlusion) Versus Steady-State Changes in Mean Circulating Volume

	E _{es} (mm Hg/ml)	M _{SW} (mm Hg)	dP/dt _{max} at matched V _{ed} (mm Hg/sec)
Native aorta			
Acute	5.47±2.3	65.35±11.11	1,471.41±483.14
Steady state	6.44±3.0	77.08±19.1	1,400.56±495.48
Tygon aorta			
Acute	7.80±5.1	76.0±24.39	1,374.71±493.25
Steady state	6.21±2.2	88.08±26.1	1,702.54±638.69

E_{es}, slope of end-systolic pressure–volume relation; M_{SW}, slope of stroke work–end-diastolic volume relation; V_{ed}, end-diastolic volume.

All the indexes demonstrated statistically similar results from both acute-load vs. steady-state load alteration methodologies. The comparisons were not statistically significant by paired t test with Bonferroni correction for multiple testing.

TABLE 4. Myocardial Oxygen Consumption Versus Pressure-Volume Area Relations with Native and Tygon Aortas

Dog No.	M \dot{V} O ₂ -PVA relation		<i>r</i>	<i>p</i>
	Slope ($\times 10^{-5}$)	Intercept ($\times 10^{-2}$)		
Native aorta				
1	1.45	1.50	0.932	0.021
2	2.76	1.83	0.994	<0.001
3	2.02	1.82	0.978	0.004
4	2.29	0.80	0.999	<0.001
5	1.45	2.49	0.996	<0.001
6	2.54	2.70	0.970	0.006
7	1.18	1.32	0.927	0.023
8	2.49	2.88	0.894	0.100
9	2.10	2.34	0.990	<0.001
Mean	2.03	1.96	0.960	
SD	0.57	0.69	0.038	
Tygon aorta				
1	1.33	1.28	0.954	<0.001
2	1.69	4.17	0.991	0.009
3	1.92	1.83	0.956	0.190
4	2.86	1.62	0.996	0.004
5	1.82	2.11	0.981	<0.001
6	2.49	2.41	0.975	0.005
7	1.49	-0.26	0.980	0.020
8	2.71	1.86	0.992	0.007
9	2.22	2.68	0.989	<0.001
Mean	2.06	1.97	0.970	
SD	0.54	1.18	0.015	

M \dot{V} O₂, myocardial oxygen consumption; PVA, pressure-volume area; *r*, correlation coefficient; *p*, *p* value for regression *F* test.

There is no statistically significant difference between sets of relations.

switching from the native to the Tygon aorta. This was found in nearly all the animals (Table 4). M \dot{V} O₂-PVA relations were also analyzed by multiple regression, which revealed an insignificant effect of aorta type on overall regression variance (*p*=0.71). The mean pooled regression relation based on all 92 points from the 18 runs was as follows: M \dot{V} O₂=2.04 $\times 10^{-5}$ ·PVA+0.019 (*p*<0.0001, multiple *r*=0.993, SEE=0.0025).

Steady-state myocardial efficiency was determined in two ways. One was the ratio of ventricular external work to M \dot{V} O₂ (both converted to joules). Increased vascular stiffness reduced this efficiency from 22.8% to 17.6% (*p*=0.052). This ratio, however, is load dependent, whereas the inverse slope of the M \dot{V} O₂-PVA relation provides a relatively load-insensitive measure of chemo-mechanical efficiency.¹⁶ Switching to the Tygon conduit did not alter this latter efficiency (35.5 \pm 11.2% for native aorta versus 34.4 \pm 9.13% for Tygon aorta, *p*=NS).

Although cardiac efficiency was little altered, the energetic costs to the heart for delivering a given SV (or cardiac output) were significantly increased when flow was directed via the stiff conduit. An individual example of the relation between SV and M \dot{V} O₂ is shown in Figure 5A. SV and M \dot{V} O₂ were linearly correlated (mean correlation coefficient, 0.93 \pm 0.06) in both native and Tygon

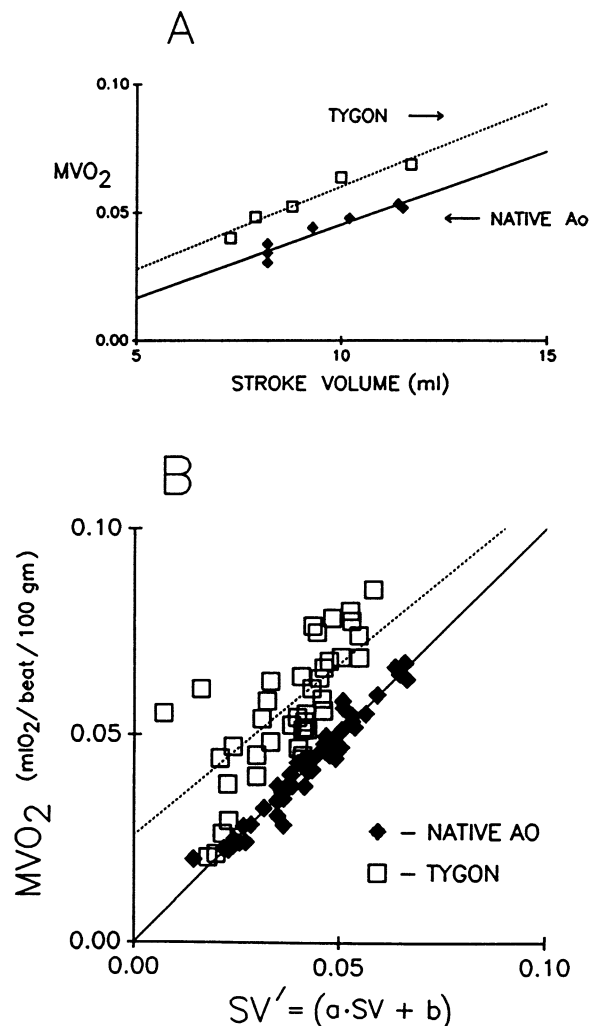


FIGURE 5. Panel A: Graph showing the relation between myocardial oxygen consumption (MVO₂) and stroke volume (SV) for the control aorta (native Ao) versus the Tygon aorta. Data are from one animal. Switching to the stiffer (Tygon) aorta increased the MVO₂ at any given SV. Since heart rate was essentially constant, this translates to an increase in oxygen demand to maintain a given cardiac output. Panel B: Graph showing group data of MVO₂-SV' relation, with SV' = (a·SV + b), where a is the slope and b is the y intercept. Data were first normalized so that the control relations lay along the line of identity (statistical variance is still maintained by this procedure), enabling the relative changes with the change to the Tygon conduit to be graphically displayed on a single plot. The results show a clear consistent upward shift with the stiffer (Tygon) "aorta," with an increased MVO₂ required at any given SV.

aortic flow conditions, but M \dot{V} O₂ was greater at any given SV (upward shift of this relation) when flow was directed through the stiff aorta.

Group results are shown in Figure 5B. To graphically combine data, linear fits to the native aorta data (MVO₂=a·SV+b, where a is the slope and b is the y intercept) were used to generate a new variable, SV'=a·SV+b, and the same equation was then applied to both native and Tygon aorta data for each animal respectively. The MVO₂-SV' points fell about the iden-

tity line for native aorta data, whereas the Tygon data were normalized to this control relation and thus demonstrated relative shifts due to the stiffer vasculature (Figure 5B). The group results were similar to the result shown in the individual example of Figure 5A. Multiregression analysis of the raw data yielded the mean relation

$$\dot{M}\dot{V}O_2 = -0.034 + 6.13 \times 10^{-3} \cdot SV + 1.11 \times 10^{-2} \cdot G$$

where G is a grouping variable ($G=0$ for native aorta, $G=1$ for Tygon aorta), with all coefficients significant at $p < 0.001$. Thus, for a typical SV (15 ml, from mean cardiac output/heart rate; see Table 1), flow through a stiff vasculature required 20% more $\dot{M}\dot{V}O_2$. The range of increased $\dot{M}\dot{V}O_2$ spanned 15–41%, depending on the baseline SV .

Discussion

This study investigated the effects of left ventricular ejection into a stiff vascular system on in vivo systolic mechanics and energetics. Aortic input impedance and central arterial pressure and flow analyses demonstrated that redirecting flow from the native thoracic aorta through a stiff conduit markedly lowered total compliance, increased characteristic impedance, and only slightly changed total mean resistance. These loading changes are similar to those observed in human aging studies.^{1–9} Interestingly, this marked vascular load change did not significantly alter indexes of chamber systolic function or efficiency based on analysis of pressure–volume and $\dot{M}\dot{V}O_2$ –PVA relations. However, the cardiac energetic cost of delivering a given SV increased by 20–40%. This suggests a mechanism whereby vascular stiffening in humans may yield little functional decrement at rest but limit reserve capacity under stress conditions.

Myocardial Energetics

Two prior in vivo studies reported $\dot{M}\dot{V}O_2$ changes after primary reductions in arterial compliance, one directly by means of a left and right heart bypass preparation²² and the other by radiolabeled microspheres.²³ In both instances, the results were variable and inconclusive. To our knowledge, the present study provides the first demonstration that ejection into a stiff vasculature results in a significant change in $\dot{M}\dot{V}O_2$. There are several potential sources for the observed increase including 1) a positive inotropic effect from the increased arterial load, analogous to an Anrep effect, 2) an intrinsic reduction in the efficiency of chemomechanical energy transduction, or 3) a corresponding increase in total cardiac work. The present results favor the latter mechanism since none of the indexes of systolic function or chamber efficiency were significantly altered by the switch to the stiff aortic conduit. Instead, the increase in $\dot{M}\dot{V}O_2$ was appropriate to the elevated total PVA.

As suggested by isolated heart data,¹⁵ it is unlikely compliance reduction itself explained the increase in resting PVA (and $\dot{M}\dot{V}O_2$). Rather, in vivo compensatory mechanisms such as a small rise in V_{ed} likely played an important role. V_{ed} change could not be precisely determined from the present data, since the volume offset (parallel conductance) of the catheter signal was not measured. However, end-diastolic pressure rose signif-

icantly (Table 1), and there was a suggestion that $V_{ed} - V_o$ also increased. Another factor that could have contributed to the PVA increase was the small elevation in mean total resistance. The exact cause for this change is unclear but is likely related in part to increased reactive load from the Tygon tubing and its connections, indicated by the rise in characteristic impedance.

There have been many prior investigations of the relation between $\dot{M}\dot{V}O_2$ and PVA, most conducted in isolated canine hearts. First described by Suga and colleagues,^{16–18} this relation has been repeatedly found to be little influenced by altered ejection history or loading (even when hearts are filled during systole²⁹). However, we recently reported that increasing afterload resistance in isolated hearts (at constant compliance and characteristic impedance) results in a lowering of efficiency (greater $\dot{M}\dot{V}O_2$ –PVA relation slope) as well as reduction in ESPVR slope.¹⁹ Central to these phenomena were changes in the extent of ejection, or the effective ejection fraction ($SV/[V_{ed} - V_o]$), that accompanied altered resistance load. There was a direct correlation between decreased effective ejection fraction and lowered efficiency. In the present study, the largely pulsatile loading changes induced by the Tygon conduit resulted in little change in the effective ejection fraction (from 50% to 43%, $p = NS$). This is consistent with the observed insignificant effects on the $\dot{M}\dot{V}O_2$ –PVA relation.

The relation between SV and $\dot{M}\dot{V}O_2$ is not an “efficiency” per se, in that SV cannot be expressed in energy units. However, it is a relevant measure of the cardiac costs of delivering a given systemic flow when the vasculature is stiffened, and the present data showed that this could be substantial. Despite additional $\dot{M}\dot{V}O_2$ requirements, systolic function was not depressed as might result from an O_2 supply/demand imbalance. However, the present study was conducted in normal canine hearts. Human diseases in which arterial stiffening occurs are often associated with coronary artery stenoses (from atherosclerosis) or cardiac hypertrophy (from hypertension or arteriosclerosis). It remains possible that under these conditions, in which the baseline cardiac supply/demand balance is already compromised, vascular stiffening could have far more profound effects.

Two other aspects of the $\dot{M}\dot{V}O_2$ – SV relation deserve comment. It was obtained by varying preload at a presumed fixed afterload impedance. Certainly, a very different relation would result if afterload resistance were primarily altered. The similarity of pressure–volume loop shape despite preload reduction (Figure 4) indicates that the dominant characteristics of impedance loading for both native and Tygon aortas were fairly constant during volume reduction. However, some load dependence of both compliance and reflected waves was certainly present.³⁰ This likely contributed to the apparent negative offset constant for the $\dot{M}\dot{V}O_2$ – SV relation (i.e., zero $\dot{M}\dot{V}O_2$ at a positive SV). This result based on linear extrapolation suggests that the true relation is nonlinear at low volumes. In addition to volume (or mean pressure) dependence of vascular impedance load, ESPVR curvilinearity could play a role.

Systolic Function

The ESPVR was first described to be little influenced by varying impedance loads¹⁵; however, subsequent

studies have revealed influences of ejection history. Several investigators described negative effects of ejection³¹⁻³³ related to the overall extent, rate, and pattern of shortening. More recent isolated heart studies^{19,34,35} have reported positive effects of ejection. In vivo studies have reported either leftward ESPVR shifts with little slope change accompanying afterload resistance increase³⁵ or significant differences in slope depending on load intervention³⁶ (preload versus afterload). No prior study has compared in vivo ESPVRs for which, primarily, the pulsatile components of aortic input impedance rather than mean peripheral resistance were increased.

The lack of significant change in the ESPVR in the present study is remarkable and suggests that the pattern of ejection (i.e., the rate of flow and pressure changes) may be a less critical determinant of in vivo systolic function than is the total extent or average rate of ejection. This result is further supported by the lack of change in the SW- V_{ed} relation or dP/dt_{max} at matched V_{ed} . While the SW relation is anticipated to change with marked alterations in afterload impedance,³⁷ this, if anything, would decrease the slope. Yet the average direction of this slope was toward a small increase. It is also worth noting that SV (and thus cardiac output) was little influenced despite the marked reduction in compliance and increase in characteristic impedance. This is consistent with data reported in isolated canine hearts ejecting into a simulated three-element Windkessel model³⁸ and points out the relatively minor impact of high-frequency components of the impedance spectrum on integrated parameters such as SV.

Comparison With Prior Models of Arterial Stiffening

Experimentally altering the elastic properties of the thoracic aorta is difficult, and results may partially depend on the method used. A classic study by Salisbury et al²² used an entirely artificial hydraulic Windkessel model in an isolated in situ heart preparation. Unfortunately, these preparations often introduce bizarre wave reflections, so that the "arterial" waveforms are not realistic, even though calculations of mean resistance or capacitance may be reasonable. Urschel et al²⁰ bypassed only the descending aorta (by a glass tube), leaving a substantial portion of the total vascular capacitance (the proximal ascending aorta and aortic root) intact. This same limitation applies to the study of O'Rourke,²¹ who "stiffened" the descending aorta by attaching Lucite to the outer surface. In contrast, Randall et al²³ placed an endotracheal tube within the lumen of the ascending aorta, and by inflating or deflating the cuff balloon, directed flow either around or solely within the tube. Whereas this approach reduced the extent of residual aortic compliance (reduction varied from 30% to 60%), it also introduced a sudden diameter change when the cuff was inflated and thus an acute impedance mismatch.

The present preparation was certainly invasive, yet by attention to a number of key factors, reasonably physiological data were obtained. The Dacron anastomosis was sutured to the ascending aorta so that much of the thoracic aortic compliance was bypassed. The experiment was designed so that the real native aorta and the stiff Tygon aorta could be studied in the same animal. Finally, circulatory pressures, cardiac outputs, and systolic and diastolic function were maintained in a phys-

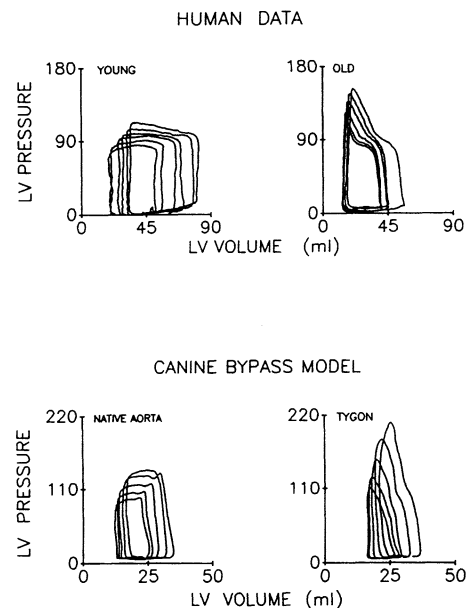


FIGURE 6. Left ventricular (LV) pressure-volume loops obtained from a normal young patient (aged 19 years) and an older hypertensive patient (aged 55 years) compared with the canine bypass model of the present study with flow through the normal versus the Tygon aorta. Flow through the native canine aorta produced data very similar to that typically seen in young human subjects with compliant vasculatures. In contrast, the older patient demonstrates late systolic peaking, which was well simulated by the flow through the Tygon conduit.

iological range. Evidence supporting the realistic nature of the preparation is found in comparison to human data obtained in young versus old hypertensive subjects (Figure 6). These clinical examples were determined by similar conductance catheter methods, with preload transiently altered by temporarily occluding the inferior vena cava with a balloon catheter. The young patient displays a "square" shape pressure-volume loop, whereas the older hypertensive subject displays a marked late systolic peaking of the pressure-volume loop. Below this figure is an example from the present canine study with native versus Tygon aortas. The similarities are striking, suggesting that, despite its invasiveness, the present model provides a clinically relevant method for assessing the influence of vascular stiffness on ventricular mechanics and energetics.

Limitations

It has been suggested that, in addition to compliance changes, alteration in the timing and intensity of wave reflections may contribute to impaired cardiac function^{4,6} with ejection into a stiff vasculature. Although the aortic bypass preparation in the present study primarily altered aortic compliance, increased wave reflections could also have played a role. However, it is difficult, if not impossible, to separately control or quantify these two factors in vivo. Diastolic reflections, which were often present in the native aorta data, complicated compliance estimations. Our results using the area method of Liu et al²⁷ likely overestimated total vascular compliance when the entire diastolic period

was used and underestimated it when only late declining pressures were analyzed. However, even the lower estimate was somewhat greater than previously reported.^{23,30} Two other factors that likely contributed to this are the large dog size used to facilitate the surgical preparation and the effects of sympathetic withdrawal due to hexamethonium-induced autonomic blockade.

An important caveat to this study is the fact that the switch to a stiff conduit was done acutely. In states of chronic vascular stiffening, left ventricular hypertrophy may have an important influence on cardiac efficiency. The increase in $\dot{M}V\text{O}_2$ may be affected by concomitant left ventricular hypertrophy-related changes in contractility. Furthermore, the extent to which increased oxygen demand imposed by a stiff vasculature can be met by augmented coronary perfusion is anticipated to be more severely limited with left ventricular hypertrophy.

In isolated heart studies, the right ventricle is vented, and thus unloaded independent of the left ventricle, making the calculation of left ventricular $\dot{M}V\text{O}_2$ more direct. Since we did not use a right heart bypass in situ, the amount of left heart oxygen use was estimated by the ratio of left ventricular to total ventricular mass. This assumes that the relative proportion of O_2 consumption between ventricles remains constant independent of volume loading. Errors in this assumption would result in slightly different slopes and offsets for the $\dot{M}V\text{O}_2$ -PVA relations from those obtained in isolated hearts,¹⁹ although the present values are consistent with several prior studies.¹⁶⁻¹⁸ With respect to the change from native to Tygon aorta, the Tygon aorta might have loaded the left heart more than the right, making the energetic costs somewhat greater than we calculated. This effect could slightly lower the efficiency during ejection into the Tygon aorta and shift the $\dot{M}V\text{O}_2$ -SV relation further upward.

Finally, we did not estimate the parallel conductance offset of the volume catheter signal, because this adds complexity and potential instability to the preparation, and it was not required for most aspects of the mechanical or energetic analyses. It remains possible, however, that small volume shifts in the ESPVR or $\text{SW}-V_{\text{ed}}$ relations were obscured by changes in the parallel offset. Countering this are the similar results obtained from the transient preload reduction data (Table 3), which were obtained quickly and temporally closer together (native versus Tygon aorta), making parallel conductance change less likely.

Summary

Vascular changes with aging and hypertension have been extensively studied in humans, and there is continued speculation that vascular stiffening poses adverse conditions for the heart. The present study shows that in normal hearts, the effects on contractile function and efficiency are minimal. These data mark an important step toward understanding how the aging vasculature may change cardiac performance and energetics. As demonstrated in Figure 6, the model reproduces many of the pressure-volume characteristics observed in humans, and the compliance reduction achieved is consistent with estimates from human aging studies.⁷ Future investigations will need to examine specifically the interactions between pulsatile loading and diseased

hearts, where clinical limitations are most likely to be observed.

Acknowledgments

The authors greatly appreciate the surgical assistance of Alfred Casale, who helped us develop the preparation, and the excellent technical assistance of Xian-Duan Li and John Kane. We also thank Shegiki Morita for his very helpful surgical tips.

References

- Carlson RG, Lillehei CW, Edwards J: Cystic medial necrosis of the ascending aorta in relation to age and hypertension. *Am J Cardiol* 1970;25:411-415
- Merillon JP, Motte G, Masquet C, Azancot I, Guiomard A, Gourgon R: Relationship between physical properties of the arterial system and left ventricular performance in the course of aging and arterial hypertension. *Eur Heart J* 1982;3:95-102
- Lakatta EG, Mitchell JH, Pomerance A, Rowe G: Human aging: Changes in structure and function. *J Am Coll Cardiol* 1987;10:42A-47A
- Nichols WW, O'Rourke MF: Aging, high blood pressure and disease in humans, in *McDonald's Blood Flow in Arteries*, ed 3. Baltimore, Md, Edward Arnold Publishers, Ltd, 1990, pp 398-420
- Murgo JP, Westerhof N, Giolma JP, Altobelli SA: Aortic input impedance in normal man: Relationships to pressure waveforms. *Circulation* 1980;62:105-116
- Nichols WW, O'Rourke MF, Avolio AP, Yaginuma T, Murgo JP, Pepine CJ, Conti CR: Effects of age in ventricular/vascular coupling. *Am J Cardiol* 1985;55:1179-1184
- Avolio AP, Chen SG, Wang RP, Zhang CL, Li MF, O'Rourke MF: Effects of age on changing arterial compliance and left ventricular load in a northern Chinese urban community. *Circulation* 1983;68:50-58
- Merillon JP, Fontenier GJ, Lerallut JF, Jaffrin MY, Motte CA, Genain GP, Gourgon RR: Aortic input impedance in normal man and arterial hypertension: Its modification during changes in aortic pressure. *Cardiovasc Res* 1986;16:646-656
- Avolio AP, Deng FQ, Li WQ, Luo YF, Huang ZD, Xing LF, O'Rourke MF: Effects of aging on arterial distensibility in populations with high and low prevalence of hypertension: Comparison between urban and rural communities in China. *Circulation* 1985;71:202-210
- Kelly R, Hayward C, Avolio A, O'Rourke M: Non-invasive determination of age-related changes in the human arterial pulse. *Circulation* 1989;80:1652-1659
- Ting CT, Brin KP, Lin SJ, Wang SP, Chang MS, Chiang BN, Yin FCP: Arterial hemodynamics in human hypertension. *J Clin Invest* 1986;78:1462-1471
- Carroll JD, Shroff S, Wirth P, Halsted M, Rajfer SI: Arterial mechanical properties in dilated cardiomyopathy. *J Clin Invest* 1991;87:1002-1009
- Weisfeldt ML, Lakatta EG, Gerstenblith G: Aging and cardiac disease, in Braunwald E (ed): *Heart Disease*, ed 3. Philadelphia, Pa, WB Saunders Co, 1988
- Yin FCP: The aging vasculature and its effects on the heart, in Weisfeldt ML (ed): *The Aging Heart*. New York, Raven Press, Publishers, 1980, pp 137-213
- Maughan WL, Sunagawa K, Burkhoff D, Sagawa K: Effect of arterial impedance changes on the end-systolic pressure-volume relation. *Circ Res* 1984;54:595-610
- Suga H: Total mechanical energy of a ventricle model and cardiac oxygen consumption. *Am J Physiol* 1979;236(Heart Circ Physiol 5):H498-H505
- Suga H: Ventricular energetics. *Physiol Rev* 1990;70:247-277
- Suga H, Yamada O, Goto Y, Igarashi Y, Ishiguri H: Constant mechanical efficiency of contractile machinery of canine left ventricle under different loading conditions. *Jpn J Physiol* 1984;34:679-698
- Burkhoff D, de Tombe PP, Hunter WC, Kass DA: Contractile strength and mechanical efficiency of left ventricle are enhanced by physiological afterload. *Am J Physiol* 1991;260(Heart Circ Physiol 29):H569-H578
- Urschel CW, Covell JW, Sonnenblick EH, Ross J Jr, Braunwald E: Effects of decreased aortic compliance on performance of the left ventricle. *Am J Physiol* 1968;214:298-304
- O'Rourke MF: Steady and pulsatile energy losses in the systemic circulation under normal conditions and in simulated arterial disease. *Cardiovasc Res* 1967;1:313-326

22. Salisbury PF, Cross CE, Rieben A: Ventricular performance modified by elastic properties of outflow system. *Circ Res* 1962;11:319–328
23. Randall OS, Van Den Bos GC, Westerhof N: Systemic compliance: Does it play a role in the genesis of essential hypertension? *Cardiovasc Res* 1984;18:455–462
24. Kass DA, Yamazacki T, Burkhoff D, Maughan WL, Sagawa K: Determination of left ventricular end-systolic pressure–volume relationships in situ by the conductance (volume) catheter technique in anesthetized dogs. *Circulation* 1986;73:586–595
25. Lankford E, Kass DA, Maughan WLM, Shoukas AA: Does the parallel conductance of the volume catheter vary with the cardiac cycle? *Am J Physiol* 1990;258(*Heart Circ Physiol* 27):H1933–H1942
26. Kass DA, Maughan WL, Guo ZM, Kono A, Sunagawa K, Sagawa K: Comparative influence of load versus inotropic state on indexes of ventricular contractility: Experimental and theoretical analysis based on pressure–volume relationships. *Circulation* 1987;76:1422–1436
27. Liu Z, Brin K, Yin FCP: Estimation of total arterial compliance: An improved method and evaluation of current methods. *Am J Physiol* 1983;252:H588–H600
28. Slinker BK, Glantz SA: Multiple linear regression is a useful alternative to traditional analyses of variance. *Am J Physiol* 1988;255:R353–R367
29. Suga H, Goto Y, Yasamura Y, Nozawa T, Futaki S, Tanaka N, Uenishi M: Oxygen-saving effect of negative work in dog ventricle. *Am J Physiol* 1988;254(*Heart Circ Physiol* 23):H34–H44
30. Alexander J, Burkhoff D, Schipke J, Sagawa K: Influence of mean pressure on aortic impedance and reflections in the systemic arterial system. *Am J Physiol* 1989;257:H969–H978
31. Shroff SG, Janicki JS, Weber KT: Evidence and quantification of left ventricular resistance. *Am J Physiol* 1983;249:(*Heart Circ Physiol* 18)H358–H370
32. Vaartjes SR, Boom HBK: Left ventricular internal resistance and unloaded ejection flow assessed from pressure–flow relations: A flow-clamp study on isolated rabbit hearts. *Circ Res* 1987;60:727–737
33. Suga H, Sagawa K, Demer L: Determinants of instantaneous pressure in canine left ventricle: Time and volume specification. *Circ Res* 1980;46:256–263
34. Hunter WC: End-systolic pressure as a balance between opposing effects of ejection. *Circ Res* 1989;64:265–275
35. Sugiura S, Hunter WC, Sagawa K: Long-term versus intrabeat history of ejection as determinants of canine ventricular end-systolic pressure. *Circ Res* 1989;64:255–264
36. Freeman GL, Little WC, O'Rourke RA: The effect of vasoactive agents on the left ventricular end-systolic pressure–volume relation in closed chest dogs. *Circulation* 1986;74:1107–1113
37. Baan J, van der Velde ET: Sensitivity of left ventricular end-systolic pressure–volume relation to the type of loading intervention in dogs. *Circ Res* 1988;62:1247–1258
38. Sunagawa K, Maughan WL, Sagawa K: Stroke volume effect of changing arterial input impedance over selected frequency ranges. *Am J Physiol* 1985;248:H477–H484

Circulation Research

JOURNAL OF THE AMERICAN HEART ASSOCIATION



Effect of reduced aortic compliance on cardiac efficiency and contractile function of in situ canine left ventricle.

R P Kelly, R Tunin and D A Kass

Circ Res. 1992;71:490-502

doi: 10.1161/01.RES.71.3.490

Circulation Research is published by the American Heart Association, 7272 Greenville Avenue, Dallas, TX 75231

Copyright © 1992 American Heart Association, Inc. All rights reserved.

Print ISSN: 0009-7330. Online ISSN: 1524-4571

The online version of this article, along with updated information and services, is located on the World Wide Web at:

<http://circres.ahajournals.org/content/71/3/490>

Permissions: Requests for permissions to reproduce figures, tables, or portions of articles originally published in *Circulation Research* can be obtained via RightsLink, a service of the Copyright Clearance Center, not the Editorial Office. Once the online version of the published article for which permission is being requested is located, click Request Permissions in the middle column of the Web page under Services. Further information about this process is available in the [Permissions and Rights Question and Answer](#) document.

Reprints: Information about reprints can be found online at:
<http://www.lww.com/reprints>

Subscriptions: Information about subscribing to *Circulation Research* is online at:
<http://circres.ahajournals.org/subscriptions/>